Available online at www.sciencedirect.com

ScienceDirect

Ceramics International 40 (2014) 2029–2034

CERAMICS INTERNATIONAL

www.elsevier.com/locate/ceramint

Preparation and electrochemical characterization of flower-like $Li_{1.2}Ni_{0.17}Co_{0.17}Mn_{0.5}O_2$ microstructure cathode by electrospinning

Ji Won Min, Chul Jin Yim, Won Bin Im*

School of Materials Science and Engineering, Chonnam National University, 300 Yongbong-dong, Buk-gu, Gwangju 500-757, Republic of Korea

Received 19 June 2013; received in revised form 23 July 2013; accepted 23 July 2013
Available online 30 July 2013

Abstract

Flower-like $Li_{1.2}Ni_{0.17}Co_{0.17}Mn_{0.5}O_2$ microstructures were prepared by a simple one step low-temperature electrospinning method. The morphological changes occurred with temperature increase from 500 °C to 700 °C. Scanning electron microscopy showed that flower-like $Li_{1.2}Ni_{0.17}Co_{0.17}Mn_{0.5}O_2$ after heat treatment at 600 °C was composed of nanoplates with an open porous structure. Flower-like electrode with well-organized porous structure can be attributed to the favorable shape to facilitate the diffusion of lithium ions. Flower-like $Li_{1.2}Ni_{0.17}Co_{0.17}Mn_{0.5}O_2$ microstructures showed a high discharge capacity of 235 mA h g^{-1} during the first cycle compared to other electrode materials.

Keywords: Flower-like; Lithium ion battery; Cathode; Layered-layered; Electrospinning

1. Introduction

Lithium ion batteries (LIBs) are considered to the predominant power sources for consumer electronic devices. Although lithium ion battery is attractive power-storage devices that have high energy density and long lifetime, their energy density is generally not high enough for its commercial application, especially in electric vehicles (EVs) [1,2]. Cathode material is the source of lithium ions and greatly determines the energy storage capability of lithium-ion batteries. Therefore, to improve the energy density of lithium ion battery, a large variety of materials have been synthesized and evaluated as cathode materials with high potential and high specific capacity for LIBs. Notable among them is the lithium cobalt oxide ($LiCoO_2$) which is currently one of the most widely used cathode materials for LIBs. Meanwhile, candidates such as $LiMn_2O_4$ and $LiFePO_4$ have also been proposed and widely investigated. However, cathode materials used in current lithium ion battery deliver low theoretical capacity (~170 mA h g^{-1}), such as $LiCoO_2$, $LiMn_2O_4$, and $LiFePO_4$ etc. [3]. Lithium-rich layered oxide $xLi_2MnO_3 \cdot (1-x)LiMO_2$ (M = Ni, Co, Mn etc.) is a promising cathode material for high energy lithium ion battery, because of their ability to provide specific capacity over 200 mA h g^{-1} with an operating potential higher than 3.5 V (vs. Li/Li^+) in average [4,5].

Hence, recent investigations have revealed that lithium rich material prepared via a sol–gel, co-precipitation etc. followed by control of the particle size. However, the main disadvantages of wet methods are high cost and complicated synthetic procedure [6]. Among a variety of known synthesis processes, the electrospinning process has proven to be very promising as it is an easy method for controlling crystal growth dynamics [7–9].

In this work, we proposed a facile electrospinning approach to synthesize flower-like $Li_{1.2}Ni_{0.17}Co_{0.17}Mn_{0.5}O_2$ microstructures consisting of nanoplates with a well-organized porous structure. Influential factors including heat treatment temperature and solvent on the formation of such flower-like $Li_{1.2}Ni_{0.17}Co_{0.17}Mn_{0.5}O_2$ microstructures have been systematically investigated, and possible growth mechanisms are also proposed. In addition, the electrochemical properties of the microstructures are studied.

2. Experimental section

2.1. Synthesis

2.1.1. Fabrication of flower-like $Li_{1.2}Ni_{0.17}Co_{0.17}Mn_{0.5}O_2$ microstructures

For the preparation of nanofibers of lithium acetate dihydrate ($LiCH_3COO \cdot 2H_2O$), manganese acetate ($Mn(CH_3COO)_2 \cdot 4H_2O$),

*Corresponding author. Tel.: +82 62 530 1715; fax: +82 62 530 1699.
E-mail address: imwonbin@jnu.ac.kr (W.B. Im).

0272-8842/$ - see front matter
http://dx.doi.org/10.1016/j.ceramint.2013.07.114

nickel acetate ($Ni(CH_3COO)_2 \cdot 4H_2O$), and cobalt acetate ($Co(CH_3COO)_2 \cdot 4H_2O$) in the required molar ratio for the formation of $Li_{1.2}Ni_{0.17}Co_{0.17}Mn_{0.5}O_2$, were dissolved in *N*,*N*-Dimethylformamide (DMF). Then polyvinyl acetate (PVAc) solution was dropped slowly into the above solution with thorough stirring at room temperature for 24 h. A high voltage power supply (eS-robot®) was used to provide a high voltage at around 15–20 kV for electrospinning. Fibers were collected on an aluminum plate as a mat. Through those optimization processes, the nanofibers were heat treated at 500–700 °C for 12 h in air to eliminate the organic residues.

2.1.2. Structural and physical characterization

The thermal decomposition behavior of the precursors was examined by means of the thermogravimetric and differential scanning calorimetry analysis (TG/DSC). X-ray diffraction (XRD) data were obtained using CuKα radiation (Philips X'Pert) over the angular range $10° \leq 2\theta \leq 120°$ with a step size of 0.026°. The Rietveld refinement was made with the General Structure Analysis System (GSAS) program [10]. The particle morphologies and sizes were determined by field emission-scanning electron microscopy (FE-SEM) and high resolution transmission electron microscopy (HR-TEM). The SEM images were obtained using an S-4700 from Hitachi, and the TEM pictures were recorded using an FEI Tecnai F20 at 200 kV, in the Korea Basic Science Institute (KBSI). Fourier transform infrared (FT-IR) spectroscopy absorption spectra were recorded using an IRPresitge-21 from Shimadzu, at room temperature in the spectral range 4000–400 cm^{-1}.

2.1.3. Electrochemical characterization

The electrochemical properties of $Li_{1.2}Ni_{0.17}Co_{0.17}Mn_{0.5}O_2$ were evaluated with lithium metal as the reference electrode. Composite cathode electrodes were prepared by using a mixture of active material, conductive carbon (KETJEN black), and PTFE binder with the weight ratio of 75:10:15%. This mixture was pressed onto a stainless steel mesh and dried under vacuum at 120 °C for 12 h. A 2032 coin type cell consisting of the cathode and lithium metal anode separated by a polymer membrane together with glass fiber was fabricated in an Ar-filled glove box and aged for 12 h before the electrochemical measurements. Cells were assembled and sealed in an argon-filled glove box with the electrolyte of 1 mol/L $LiPF_6$ dissolved in a 1:1 mixture of ethylene carbonate (EC) and dimethyl-carbonate (DMC).

3. Result and discussion

The TGA/DSC curves for the mixed precursor of $Li_{1.2}Ni_{0.17}Co_{0.17}Mn_{0.5}O_2$ material were shown in Fig. 1. The TGA curve (Fig. 1(a)) for $Li_{1.2}Ni_{0.17}Co_{0.17}Mn_{0.5}O_2$ precursors with PVAc shows the weight loss of the precursor fibers terminated at 430 °C and three discrete regions of weight loss occurred at about 80, 290, and 350 °C. As observed in the DSC curve (Fig. 1(b)), small endothermic peak from room temperature to 290 °C is associated with the release of physically adsorbed water from the mixed precursor and

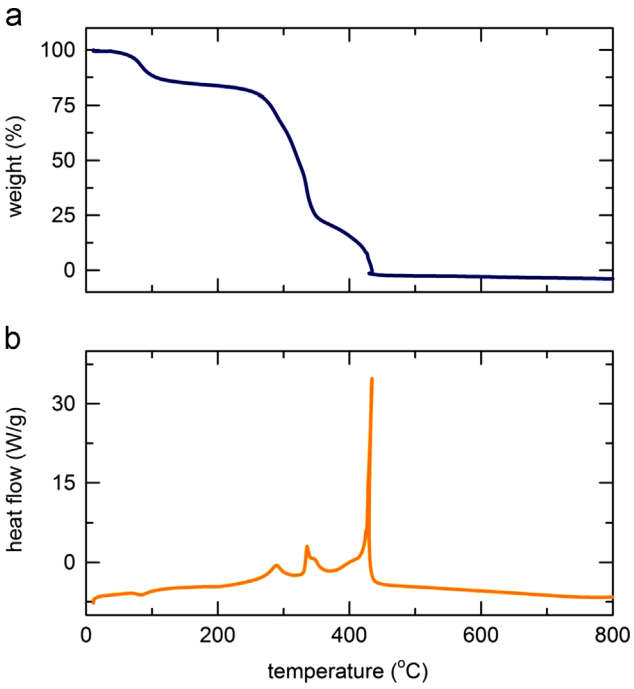

Fig. 1. Thermogravimetric and differential scanning calorimetry analyses (TG/DSC) of $Li_{1.2}Ni_{0.17}Co_{0.17}Mn_{0.5}O_2$ precursors with PVAc.

the decomposition of acetate [6]. The peak at about 350 °C was assigned to form $Li_{1.2}Ni_{0.17}Co_{0.17}Mn_{0.5}O_2$ and the degradation of PVAc by dehydration on the polymer side chain. The peak at about 430 °C was associated with the decomposition of PVAc main chain and formation of the target product [11]. At temperatures above 430 °C, there was no change in weight loss, indicating the formation of pure inorganic oxide.

Fig. 2(a) shows evolutions of X-ray diffraction patterns of electrospun $Li_{1.2}Ni_{0.17}Co_{0.17}Mn_{0.5}O_2$ phase compound at different heat treatment temperatures. The materials synthesized at 500, 600, and 700 °C. The XRD peaks for the compounds were indexed based on the α-$NaFeO_2$-type structure ($R\bar{3}m$), with small extra peaks at 20–23° corresponding integrated monoclinic Li_2MnO_3 phase ($C2/m$) generally attributed to the ordering of Li^+ ion in the transition metal layer [12]. With the rising of the heating temperatures, the degree of crystallinity increased. Although in a co-precipitation, the Li-rich material phase was formed at above 850 °C [13–15], the electrospun powders could produce the $Li_{1.2}Ni_{0.17}Co_{0.17}Mn_{0.5}O_2$ phase at a lower temperature. Fig. 2(b) shows the LeBail fitting result of the XRD profile of electrospun $Li_{1.2}Ni_{0.17}Co_{0.17}Mn_{0.5}O_2$ samples fired at 600 °C, obtained with $R_{wp}=1.72\%$ and goodness of fit parameters (χ^2)=1.86. Based on the LeBail fitting results, the initial structural models which approximate the actual structures of $Li_{1.2}Ni_{0.17}Co_{0.17}Mn_{0.5}O_2$ were constructed with the crystallographic data previously reported [16]. No impurity phases were identified in any of the samples, regardless of the firing temperatures. The cell parameters were $a=2.8513(1)$ Å and $c=14.189(4)$ Å.

Fig. 3 shows Fourier transform infrared (FT-IR) spectroscopy for $Li_{1.2}Ni_{0.17}Co_{0.17}Mn_{0.5}O_2$/PVAc fibers heated at

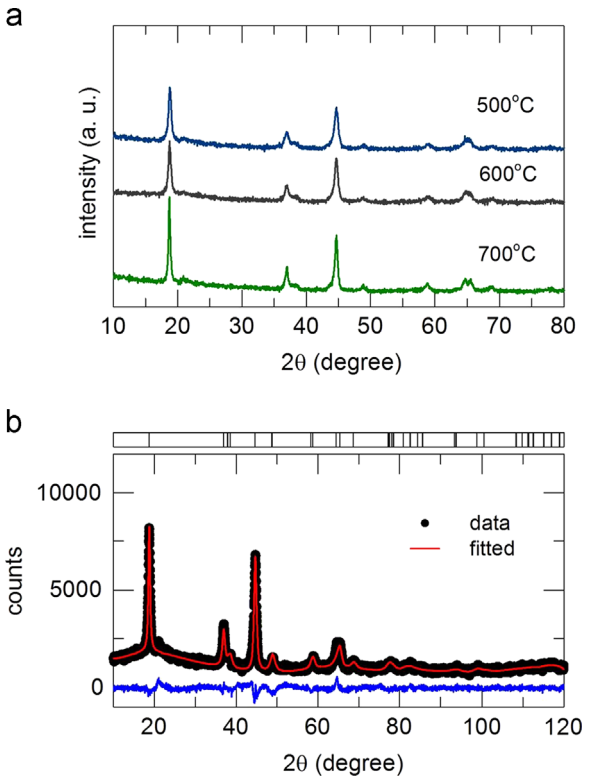

Fig. 2. (a) XRD patterns of $Li_{1.2}Ni_{0.17}Co_{0.17}Mn_{0.5}O_2$/PVAc fibers heating at 500 °C, 600 °C, and 700 °C for 12 h in the air atmosphere and (b) LeBail fitting results of the powder X-ray diffraction profile of electrospun $Li_{1.2}Ni_{0.17}Co_{0.17}Mn_{0.5}O_2$ at 600 °C. Data (points) and fit (lines) show different profile XRD patterns of $Li_{1.2}Ni_{0.17}Co_{0.17}Mn_{0.5}O_2$. Expected reflection positions for $Li_{1.2}Ni_{0.17}Co_{0.17}Mn_{0.5}O_2$ are displayed at the top.

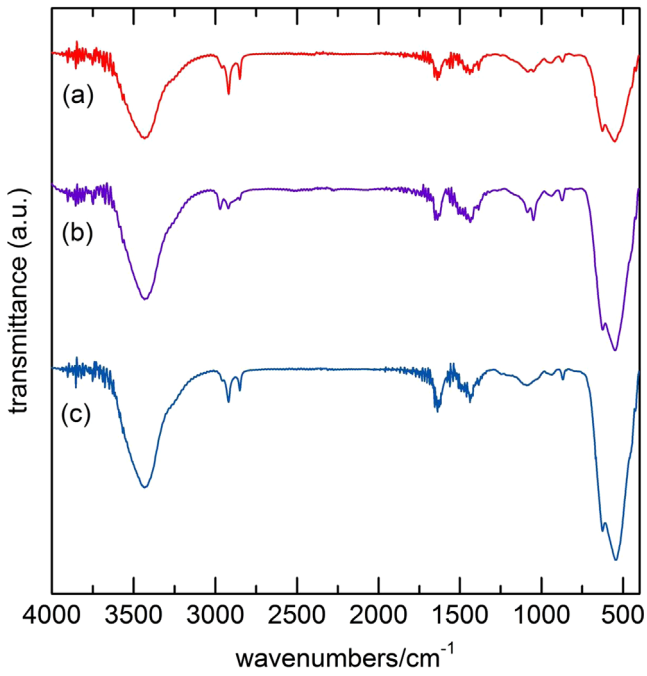

Fig. 3. FT-IR spectra of $Li_{1.2}Ni_{0.17}Co_{0.17}Mn_{0.5}O_2$/PVAc fibers heating at (a) 500 °C, (b) 600 °C, and (c) 700 °C for 12 h in the air atmosphere.

different temperatures. The FT-IR adsorption band for the metal-oxygen (M-O) of $Li_{1.2}Ni_{0.17}Co_{0.17}Mn_{0.5}O_2$ appears in the wavenumber range of 500–700 cm^{-1}, indicating the formation of inorganic targets. With the rising of the heating temperatures, the intensity of the peaks at about 621.1 and 530.4 cm^{-1} enhanced, indicating the formation of $Li_{1.2}Ni_{0.17}Co_{0.17}Mn_{0.5}O_2$ phase [17,18]. These results illustrated that the organic molecules could be removed completely from $Li_{1.2}Ni_{0.17}Co_{0.17}Mn_{0.5}O_2$/PVAc fibers when the heat treatment temperature was above 500 °C.

The morphology of the products was examined by scanning electron microscopy (SEM). Fig. 4 shows the morphological changes that occurred during the heat treatment of the precursor fibers. As shown in Fig. 4(a), the precursor fibers appeared that the diameters of the fibers were mainly around 100–300 nm, with minor of less than 80 nm. At a low temperature of 500 °C, the prepared electrospun $Li_{1.2}Ni_{0.17}Co_{0.17}Mn_{0.5}O_2$ indicates the aggregation of primary particles of size around 10–50 nm, and irregular shapes, as in Fig. 4(b). When heated at 600 °C (Fig. 4(c)), electrospun sample consists of microstructures with flower-like texture. It can be clearly seen that these flower-like microstructures are composed of many nanoplate petals with various thicknesses (Fig. 4(c)). After increasing heating temperature to 700 °C (Fig. 4(d)), the flower-like morphology could not be stained, owing to the instability of $Li_{1.2}Ni_{0.17}Co_{0.17}Mn_{0.5}O_2$ under high heating temperature. Additionally, Fig. 4(e) shows schematic illustration of the growth mechanism of flower-like $Li_{1.2}Ni_{0.17}Co_{0.17}Mn_{0.5}O_2$ microstructures.

To have a better understanding of the flower-like microstructures, detailed SEM and STEM characterizations were performed at 600°C sample, and the results are shown in Fig. 5. The SEM images (Fig. 5(a)) shows that flower-like $Li_{1.2}Ni_{0.17}Co_{0.17}Mn_{0.5}O_2$ after heating at 600 °C was composed of nanoplates with a thickness of around 20–40 nm, which interweave together forming an open porous structure. Such a well-organized porous structure is expected to facilitate electrolyte penetration into the electrode particles, thus providing more interface area between the electrode material and the electrolyte [19–21]. As shown in Fig. 5(b), the elemental mapping using STEM presents that the measured sample is approximately homogeneous in chemical composition as that of solid solution $Li_{1.2}Ni_{0.17}Co_{0.17}Mn_{0.5}O_2$.

Fig. 6 shows the electrochemical performance of the cell Li/$Li_{1.2}Ni_{0.17}Co_{0.17}Mn_{0.5}O_2$ between 2.0 V and 4.8 V at different heating temperatures under the current density of 14.3 mA g^{-1}. As seen in Fig. 6(a), all electrodes exhibit the plateau voltage of 4.5 V (vs. Li/Li^+) during the first charge process corresponding to the simultaneous release of lithium ions and oxygen [20,22,23]. Among these electrodes, the flower-like sample heated at 600 °C displays the longest plateau with the highest charge capacity of 304 mA h g^{-1}. The electrode heated at 500 °C has higher charge capacity than the electrode heated at 700 °C. Also, the flower-like sample heated at 600 °C delivers the highest discharge capacity. This result is consistent to the literature, Cheng et al. [20]. It indicates that well-organized porous structure electrode can facilitate the oxygen loss from the layered lattice, which would enhance the discharge capacities of the Li-rich layered cathode materials. As shown in Fig. 6(b), $Li_{1.2}Ni_{0.17}Co_{0.17}Mn_{0.5}O_2$ powders

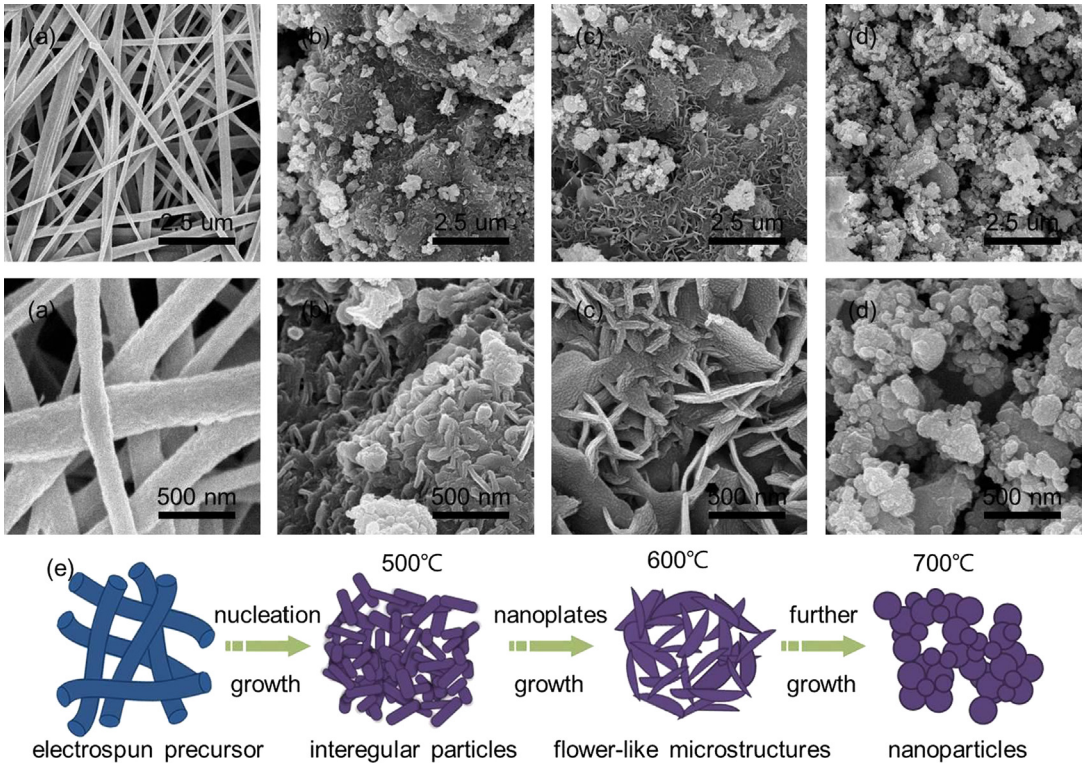

Fig. 4. SEM images of $Li_{1.2}Ni_{0.17}Co_{0.17}Mn_{0.5}O_2$/PVAc fibers (a) before with heating, heating at (b) 500 °C, (c) 600 °C, and (d) 700 °C for 12 h in the air atmosphere and (e) schematic illustration of the growth mechanism of flower-like $Li_{1.2}Ni_{0.17}Co_{0.17}Mn_{0.5}O_2$ microstructures.

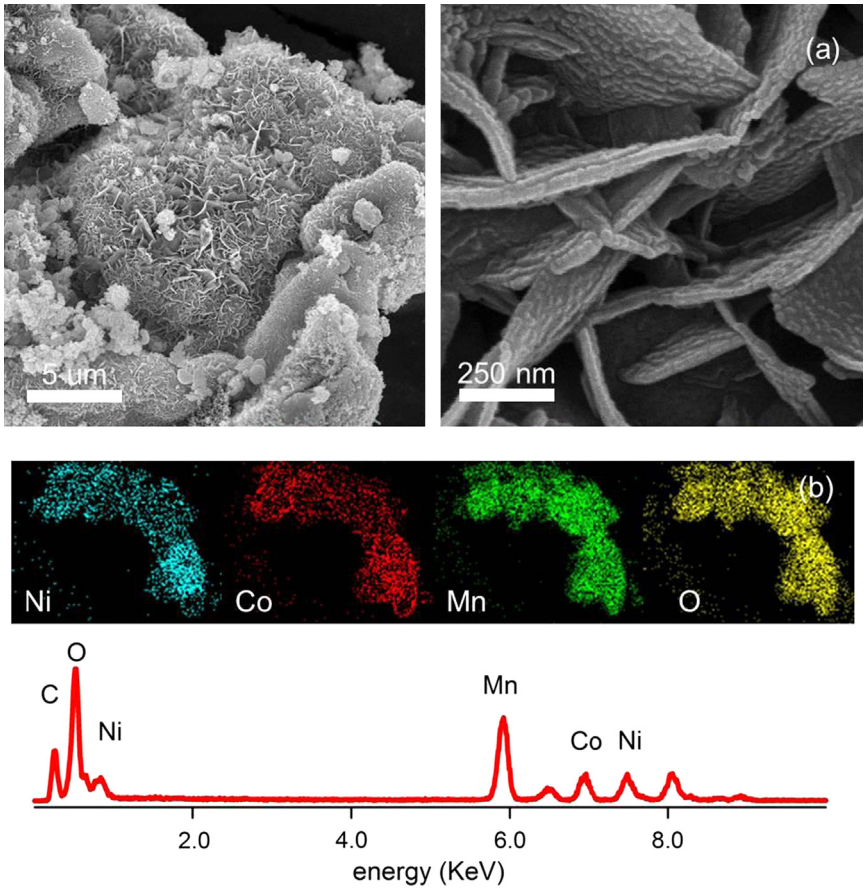

Fig. 5. (a) SEM images and (b) elemental mapping images of $Li_{1.2}Ni_{0.17}Co_{0.17}Mn_{0.5}O_2$ fibers heated at 600 °C for 12 h in the air atmosphere.

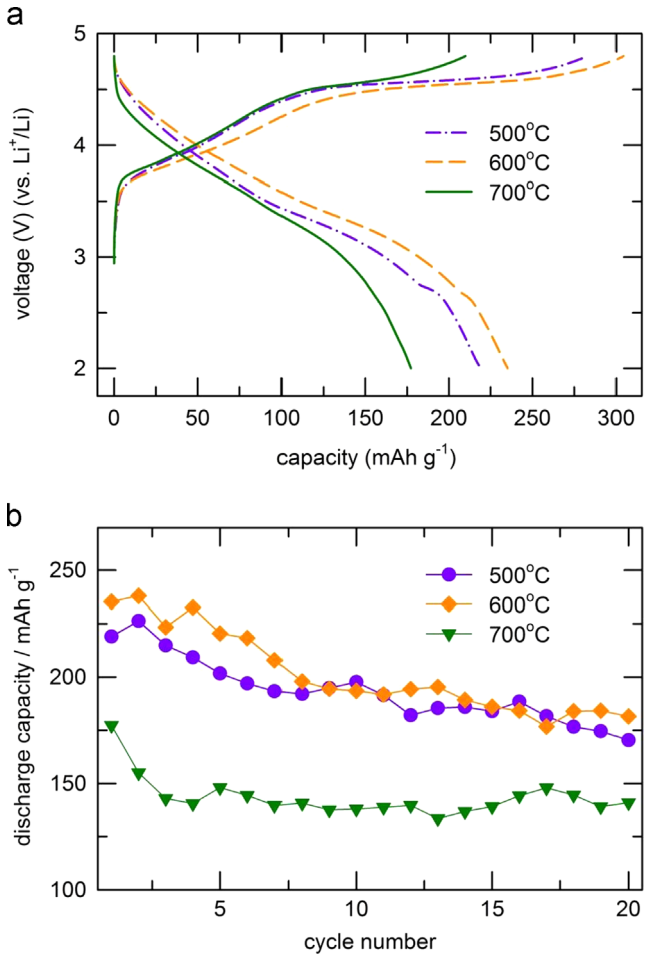

Fig. 6. (a) Voltage profiles of the samples obtained for the first cycle and (b) cyclabilities in the voltage range of 2.0–4.8 V, at a current density of 14.3 mA g^{-1}.

heated at 500 °C and 600 °C retain 77% of initial capacity at 20th cycle, while those heated at 700 °C retain 79% of it, though their initial capacity is lower. This is probably because that powders heated at higher temperature are structurally more stable than those heated at lower temperature. These results are in accordance with our XRD and FT-IR data.

4. Conclusions

For the first time, flower-like $Li_{1.2}Ni_{0.17}Co_{0.17}Mn_{0.5}O_2$ microstructures were successfully synthesized using a high-voltage electrospinning process and through heat treatment. Heat treatment temperature was critical for the morphology control of the electrospun $Li_{1.2}Ni_{0.17}Co_{0.17}Mn_{0.5}O_2$/PVAc precursor. The morphological changes occurred during the heat treatment of the precursor fibers, at 600 °C it attained flower like structure. Flower-like electrode with well-organized porous morphologies provided fast the diffusion of lithium ions, leading to enhanced lithium storage capabilities in terms of the capacity. The simple and viable synthesis method may be applicable to provide an efficient route for designing a desirable structure, which could also be extended to synthesize cathode materials for lithium-ion batteries.

Acknowledgments

This research was supported by the MKE (The Ministry of Knowledge Economy), Korea, under the ITRC (Information Technology Research Center) support program (NIPA-2013-H0301-13-1009) supervised by the NIPA (National IT Industry Promotion Agency). This research is also supported by Ministry of Education, Science Technology (MEST) and National Research Foundation of Korea (NRF) through the Human Resource Training Project for Regional Innovation.

References

[1] J.M. Tarascon, M. Armand, Issues and challenges facing rechargeable lithium batteries, Nature 414 (6861) (2001) 359–367.
[2] F. Cheng, J. Liang, Z. Tao, J. Chen, Functional materials for rechargeable batteries, Advanced Materials 23 (15) (2011) 1695–1715.
[3] J.W. Fergus, Recent developments in cathode materials for lithium ion batteries, Journal of Power Sources 195 (4) (2010) 939–954.
[4] M.M. Thackeray, S.H. Kang, C.S. Johnson, J.T. Vaughey, S.A. Hackney, Comments on the structural complexity of lithium-rich $Li_{1+x}M_{1-x}O_2$ electrodes (M=Mn, Ni, and Co) for lithium batteries, Electrochemistry Communications 8 (9) (2006) 1531–1538.
[5] H. Yu, H. Zhou, Initial Coulombic efficiency improvement of the $Li_{1.2}Mn_{0.567}Ni_{0.166}Co_{0.067}O_2$ lithium-rich material by ruthenium substitution for manganese, Journal of Materials Chemistry 22 (31) (2012) 15507–15510.
[6] Y. Xiang, Z. Yin, Y. Zhang, X. Li, Effects of synthesis conditions on the structural and electrochemical properties of the Li-rich material Li $[Li_{0.2}Ni_{0.17}Co_{0.16}Mn_{0.47}]O_2$ via the solid-state method, Electrochimica Acta 91 (0) (2013) 214–218.
[7] H. Guan, C. Shao, Y. Liu, N. Yu, X. Yang, Fabrication of $NiCo_2O_4$ nanofibers by electrospinning, Solid State Communications 131 (2) (2004) 107–109.
[8] S.W. Choi, J.R. Kim, Y.R. Ahn, S.M. Jo, E.J. Cairns, Characterization of electrospun PVdF fiber-based polymer electrolytes, Chemistry of Materials 19 (1) (2006) 104–115.
[9] A. Singhal, G. Skandan, G. Amatucci, F. Badway, N. Ye, A. Manthiram, H. Ye, J.J. Xu, Nanostructured electrodes for next generation rechargeable electrochemical devices, Journal of Power Sources 129 (1) (2004) 38–44.
[10] A.C. Larson, R.B. Von Dreele, Los Alamos National Laboratory Report, LAUR, 1994.
[11] Y.-W. Ju, J.-H. Park, H.-R. Jung, S.-J. Cho, W.-J. Lee, Fabrication and characterization of cobalt ferrite ($CoFe_2O_4$) nanofibers by electrospinning, Materials Science and Engineering B 147 (1) (2008) 7–12.
[12] M.M. Thackeray, S.H. Kang, C.S. Johnson, J.T. Vaughey, R. Benedek, S.A. Hackney, Li_2MnO_3-stabilized $LiMO_2$ (M=Mn, Ni, and Co) electrodes for lithium-ion batteries, Journal of Materials Chemistry 17 (30) (2007) 3112–3125.
[13] Y. Chen, G. Xu, J. Li, Y. Zhang, Z. Chen, F. Kang, High capacity $0.5Li_2MnO_3 \cdot 0.5LiNi_{0.33}Co_{0.33}Mn_{0.33}O_2$ cathode material via a fast co-precipitation method, Electrochimica Acta 87 (2013) 686–692.
[14] Y.-K. Sun, M.-J. Lee, C.S. Yoon, J. Hassoun, K. Amine, B. Scrosati, The role of AlF_3 coatings in improving electrochemical cycling of Li-enriched nickel–manganese oxide electrodes for Li-ion batteries, Advanced Materials 24 (9) (2012) 1192–1196.
[15] J.W. Min, J. Gim, J. Song, W.-H. Ryu, J.-W. Lee, Y.-I. Kim, J. Kim, W.B. Im, Simple, robust metal fluoride coating on layered $Li_{1.23}Ni_{0.13}Co_{0.14}Mn_{0.56}O_2$ and its effects on enhanced electrochemical properties, Electrochimica Acta 100 (2013) 10–17.
[16] N. Tran, L. Croguennec, M. Menetrier, F. Weill, P. Biensan, C. Jordy, C. Delmas, Mechanisms associated with the "Plateau" observed at high

voltage for the overlithiated $Li_{1.12}(Ni_{0.425}Mn_{0.425}Co_{0.15})_{0.88}O_2$ system, Chemistry of Materials 20 (15) (2008) 4815–4825.

[17] C.L. Shao, N. Yu, Y.C. Liu, R.X. Mu, Preparation of $LiCoO_2$ nanofibers by electrospinning technique, Journal of Physics and Chemistry of Solids 67 (7) (2006) 1423–1426.

[18] C.H. Song, A.M. Stephan, S.K. Jeong, Y.J. Hwang, A.R. Kim, K.S. Nahm, Influence of solvents on the structural and electrochemical properties of $Li[Li_{0.2}Ni_{0.1}Co_{0.2}Mn_{0.5}]O_2$ prepared by a solvothermal reaction method, Journal of the Electrochemical Society 153 (2) (2006) A390–A395.

[19] C.W. Sun, S. Rajasekhara, J.B. Goodenough, F. Zhou, Monodisperse porous $LiFePO_4$ microspheres for a high power Li-ion battery cathode, Journal of the American Chemical Society 133 (7) (2011) 2132–2135.

[20] F.Q. Cheng, Y.L. Xin, J.T. Chen, L. Lu, X.X. Zhang, H.H. Zhou, Monodisperse $Li_{1.2}Mn_{0.6}Ni_{0.2}O_2$ microspheres with enhanced lithium storage capability, Journal of Materials Chemistry A 1 (17) (2013) 5301–5308.

[21] J. Liu, D. Hu, T. Huang, A. Yu, Synthesis of flower-like $LiMnPO_4$/C with precipitated $NH_4MnPO_4 \cdot H_2O$ as precursor, Journal of Alloys and Compounds 518 (2012) 58–62.

[22] A.R. Armstrong, M. Holzapfel, P. Novak, C.S. Johnson, S.H. Kang, M.M. Thackeray, P.G. Bruce, Demonstrating oxygen loss and associated structural reorganization in the lithium battery cathode $Li[Ni_{0.2}Li_{0.2}Mn_{0.6}]O_2$, Journal of the American Chemical Society 128 (26) (2006) 8694–8698.

[23] N. Yabuuchi, K. Yoshii, S.-T. Myung, I. Nakai, S. Komaba, Detailed studies of a high-capacity electrode material for rechargeable batteries, $Li_2MnO_3-LiCo_{1/3}Ni_{1/3}Mn_{1/3}O_2$, Journal of the American Chemical Society 133 (12) (2011) 4404–4419.